Electronic Supplementary Information

An Unprecedented Azobenzene-Based Organic Single-Component Ferroelectric

Hang Peng,‡ Jun-Chao Qi,‡ Xian-Jiang Song, Ren-Gen Xiong* and Wei-Qiang Liao*

Fig. S1 The synthesis of APFA.

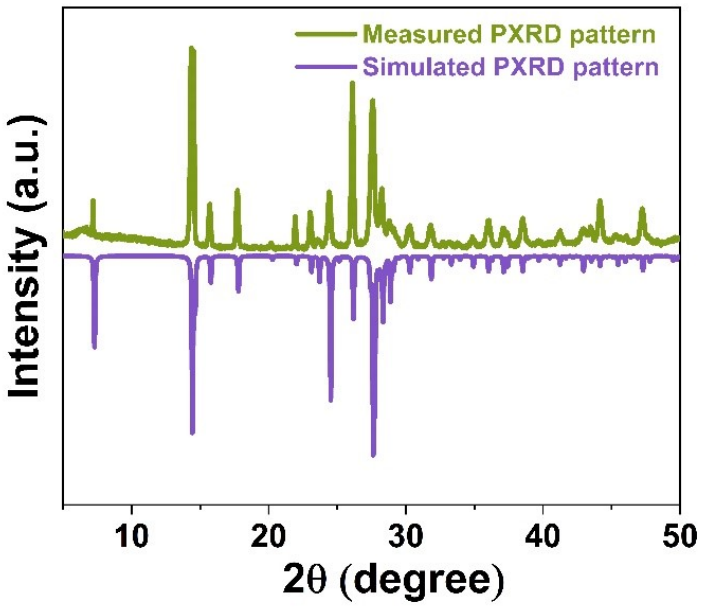

Fig. S2 The measured PXRD pattern of APFA at 298 K matches well with the simulated one, verifying the purity of the bulk phase.

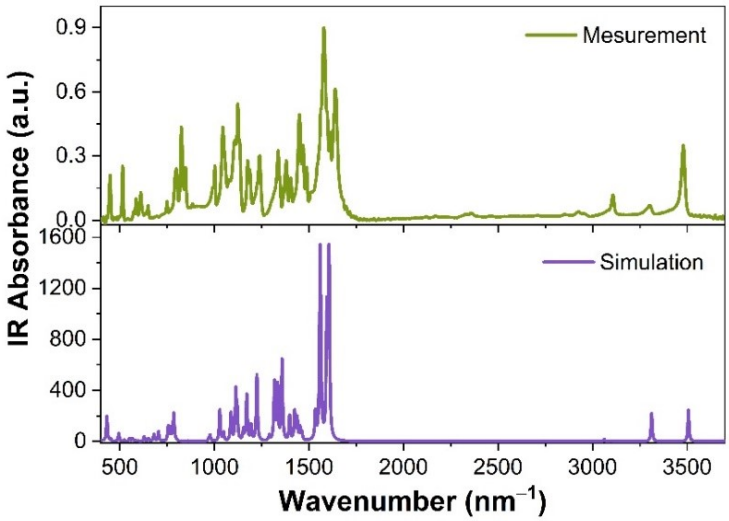

Fig. S3 Measured (top) and calculated (bottom) IR spectra of APFA.

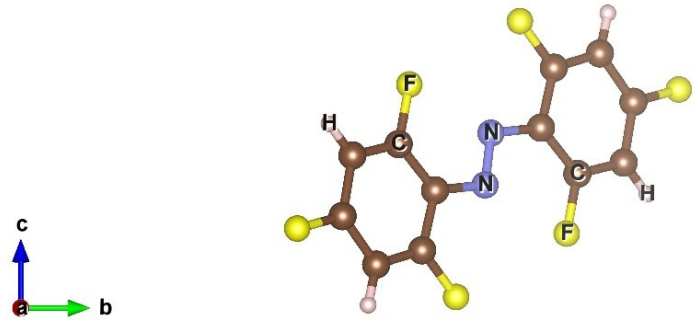

Fig. S4 Crystal structure of HFA.

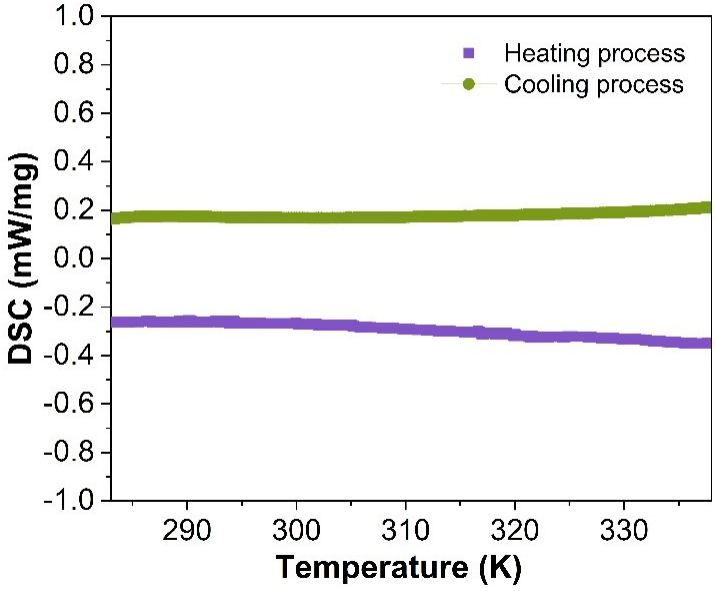

Fig. S5 DSC curve of HFA.

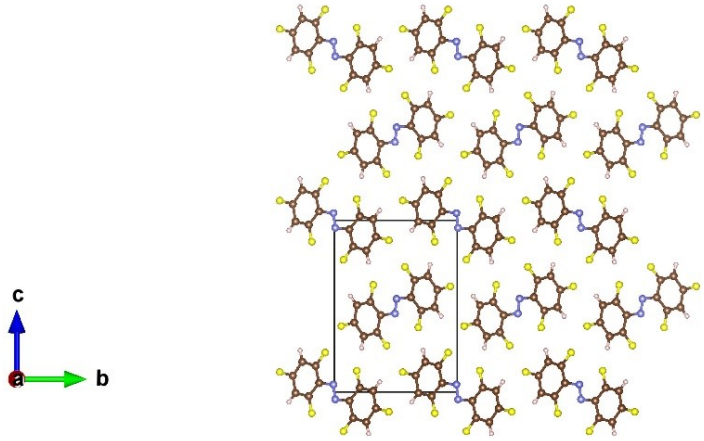

Fig. S6 Packing views of the structure of HFA at 298 K along *a* axis.

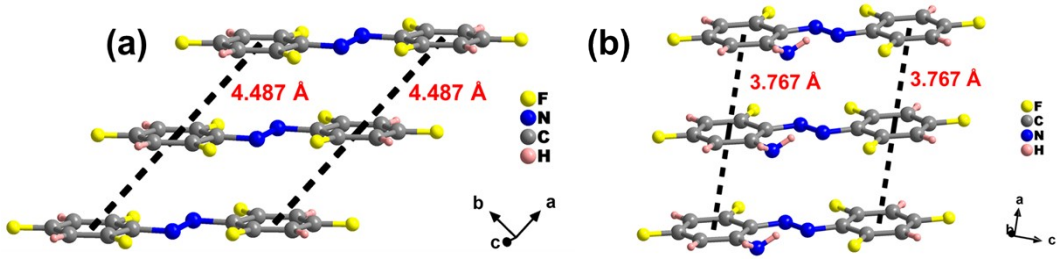

Fig. S7 The π-π interactions (dash lines) in the structures of HFA (a) and APFA (b) with the labeled π-π distances, showing the decrease of π-π distance between neighboring molecules after substitution with an amino group.

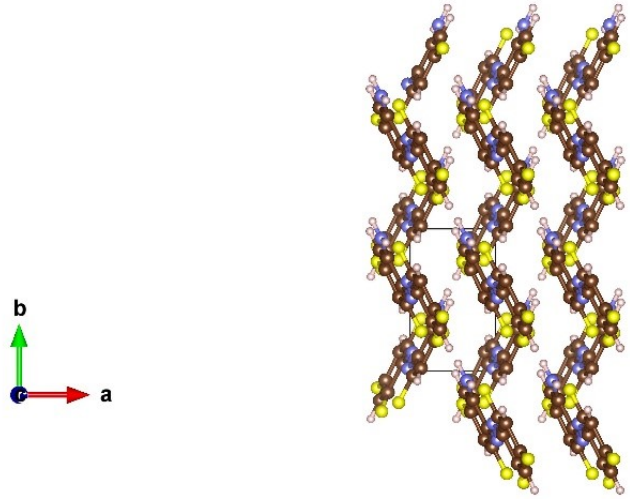

Fig. S8 Packing views of the structure of APFA at 298 K along *c* axis.

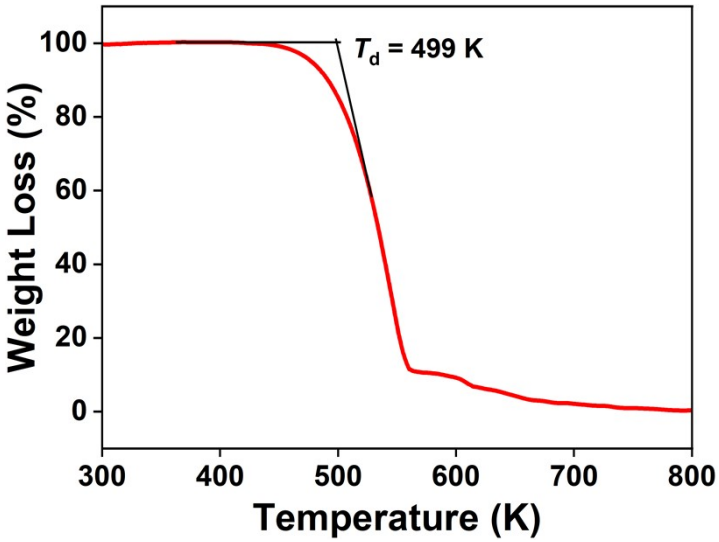

Fig. S9 TGA curves of APFA recorded from 300 K to 800 K by PerkinElmer TGA 8000 in a nitrogen atmosphere.

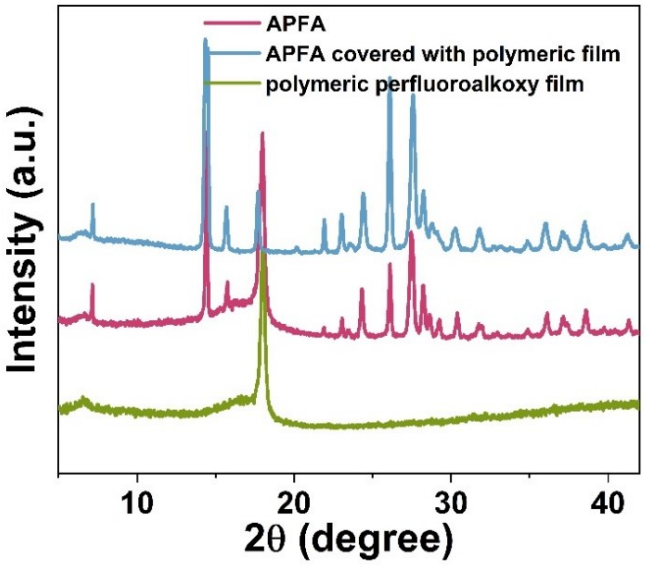

Fig. S10 PXRD patterns of APFA, APFA sample covered with the polymeric film and the polymeric perfluoroalkoxy film at 298 K.

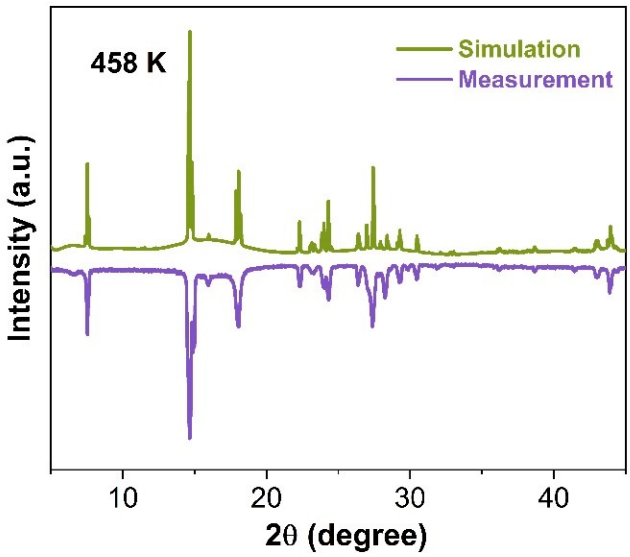

Fig. S11 Pawley refinement of PXRD data of APFA collected at 458 K with monoclinic unit cell.

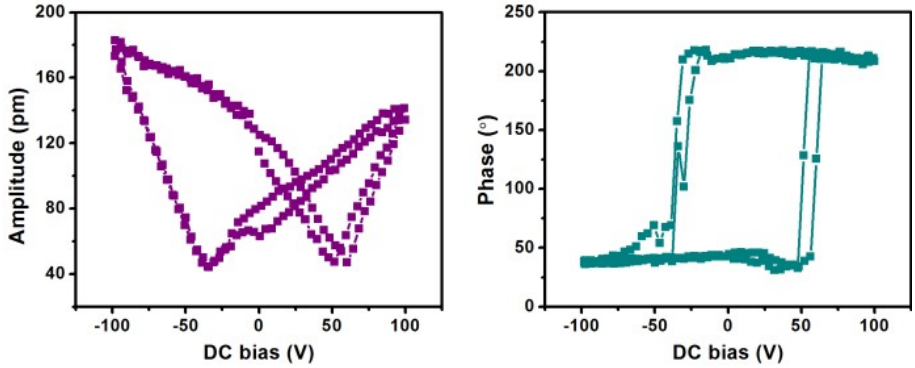

Fig. S12 The PFM switching spectroscopy measurements for the APFA thin film. PFM amplitude loops (left) and PFM phase loops (right).

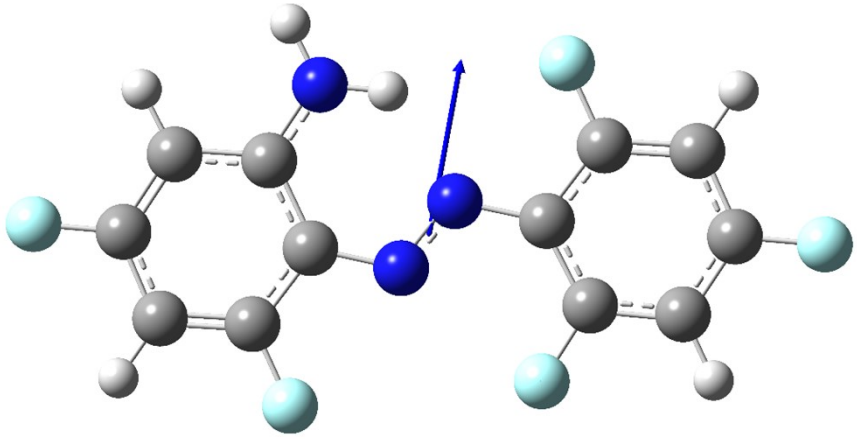

Fig. S13 The dipole moment direction of APFA molecule depicted with a blue arrow.

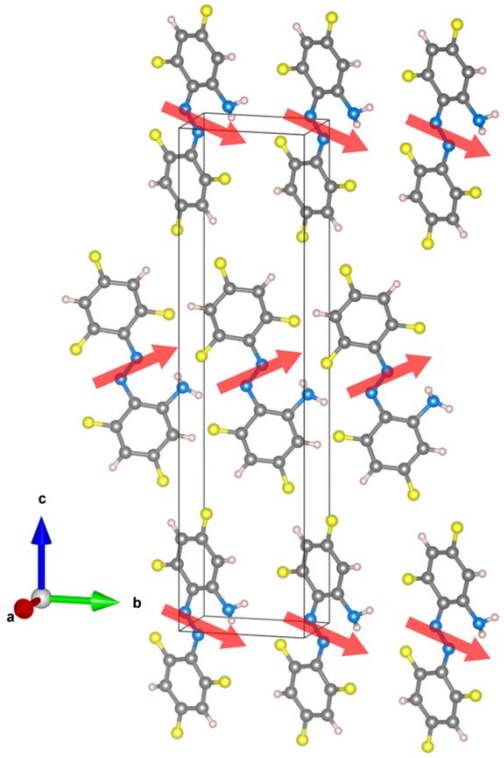

Fig. S14 Schematic diagram of the distribution of molecular dipoles in the unit cell. The red arrow represents the direction of the molecular dipole.

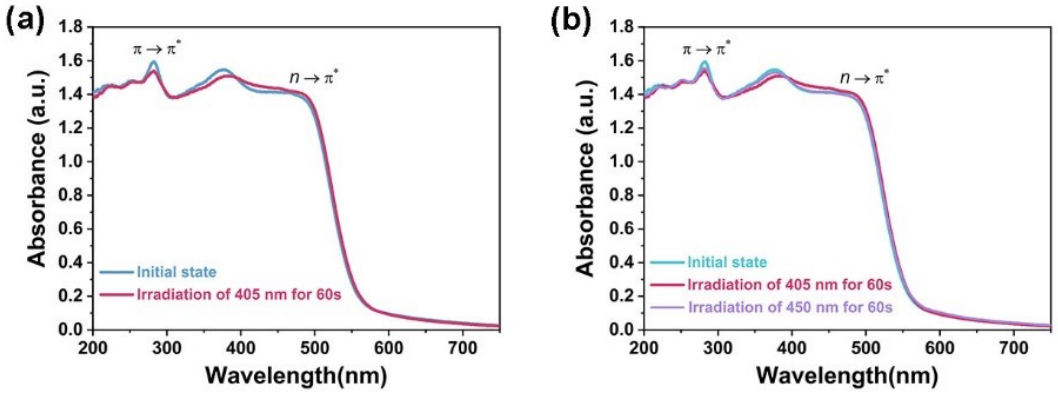

Fig. S15 Solid-state UV-Vis absorption spectra of APFA at 293 K (a) before and after the irradiation of 405 nm for 60 s and (b) after the irradiation of 450 nm for 60 s.

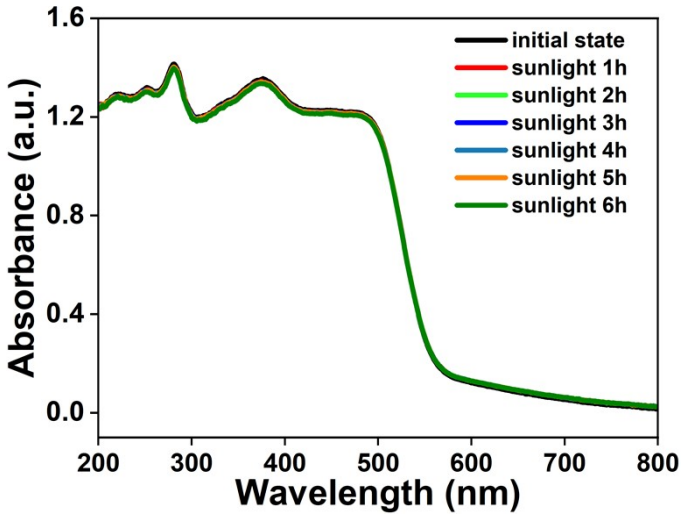

Fig. S16 Solid-state UV-vis absorption spectra of APFA recorded before and after open- air exposure under the sunlight from 1h to 6h.

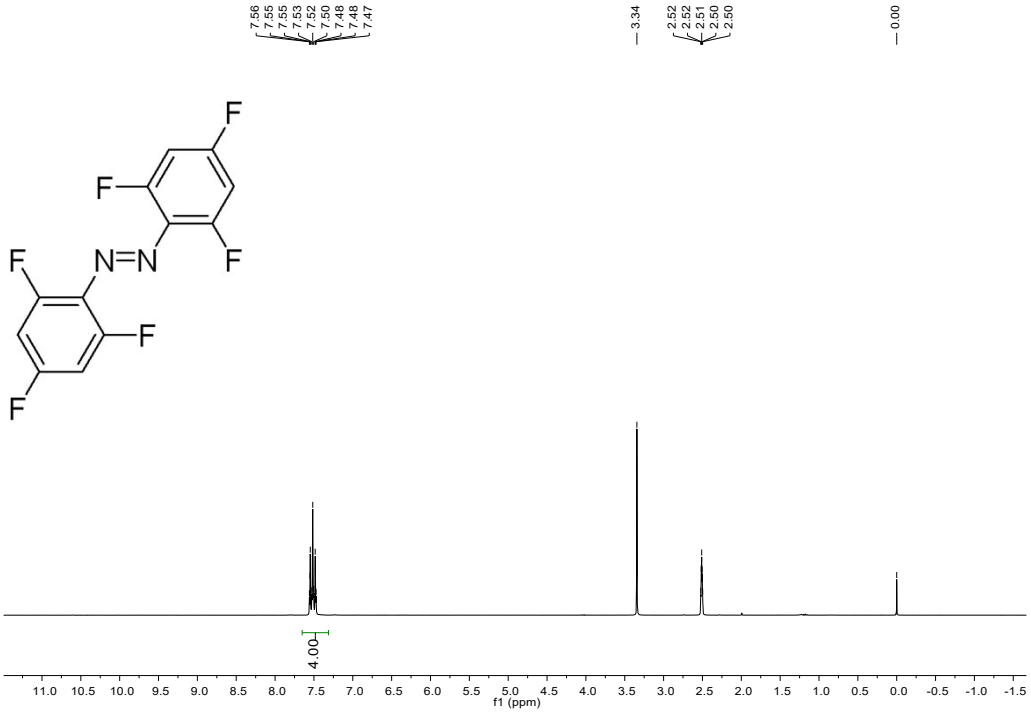

Fig. S17 ^{1}H NMR spectrum of HFA (300 MHz, DMSO-d_6).

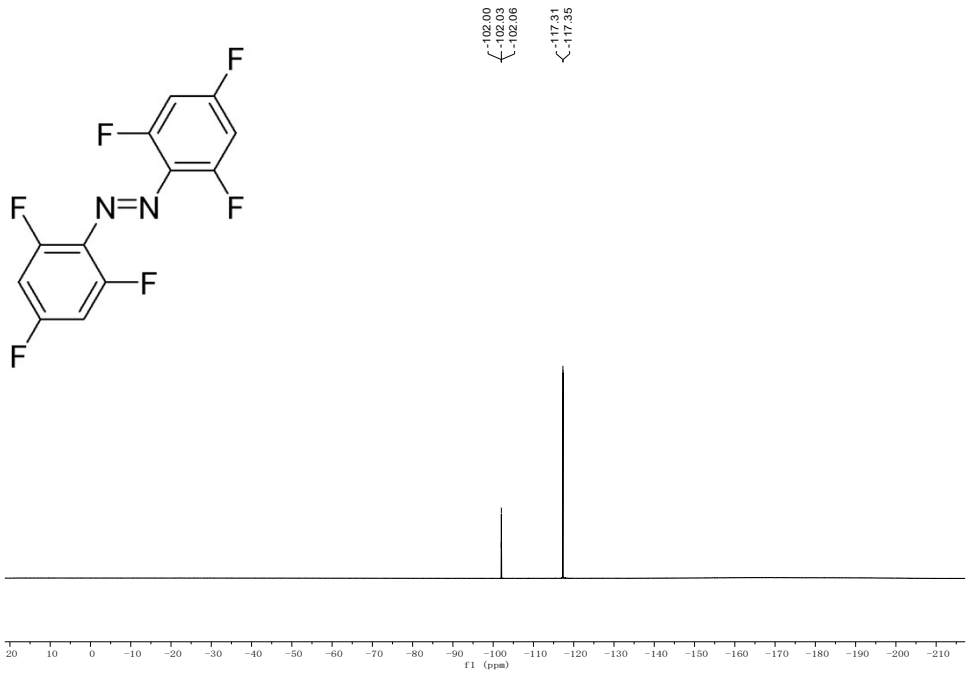

Fig. S18 ^{19}F NMR spectrum of HFA (282 MHz, DMSO-d_6).

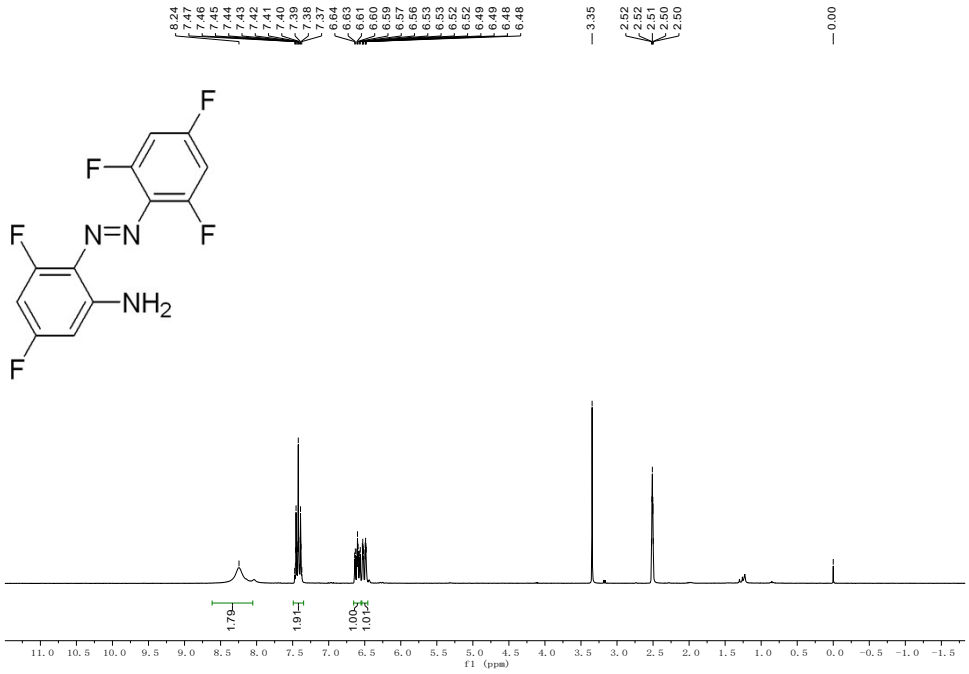

Fig. S19 ^{1}H NMR spectrum of APFA (300 MHz, DMSO-d_6).

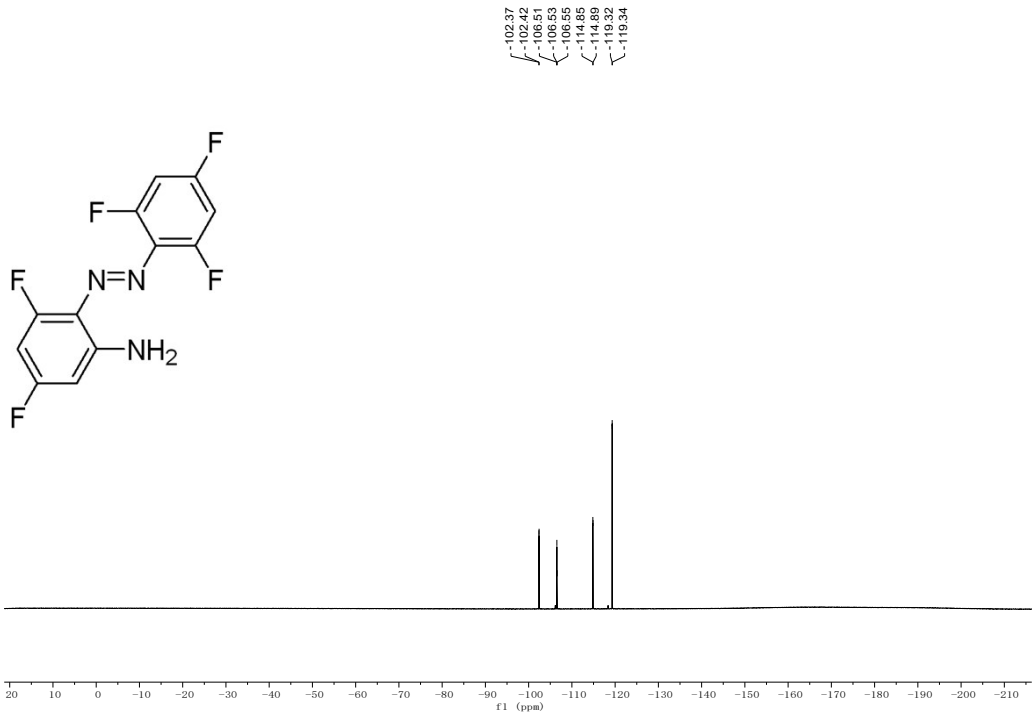

Fig. S20 ^{19}F NMR spectrum of APFA (282 MHz, DMSO-d_6).

Table S1. Crystal data and structure refinements for APFA and HFA at 298 K.

Compound	APFA	HFA
Temperature	298 K	
Formula	$C_{12}H_6F_5N_3$	$C_{12}H_4F_6N_2$
Formula weight	287.20	290.17
Crystal system	monoclinic	monoclinic
Space group	$P2_1$	$P2_1/n$
a, b, c (Å)	3.76719(12) 6.2632(2) 24.1516(7)	4.4870(3) 9.3652(6) 13.1716(8)
α, β, γ (°)	90 92.008(3) 90	90 97.270(6) 90
Volume /Å^3	569.50(3)	549.04(6)
Z	2	2
Density/g cm^{-3}	1.675	1.755
R_1	0.0539	0.0485
wR_2	0.1505	0.1165
GOF	1.124	1.018

Table S2. Bond Lengths for APFA.

Atom	**Atom**	**Length/Å**	**Atom**	**Atom**	**Length/Å**
F3	C6	1.348(7)	F2	C4	1.354(4)
F4	C8	1.342(7)	C11	C10	1.356(7)
C1	N2	1.386(4)	C5	C4	1.391(10)
C1	C6	1.369(7)	C5	C6	1.360(5)
C1	C2	1.462(7)	F1	C2	1.303(5)
C12	N3	1.376(5)	C4	C3	1.366(7)
C12	C11	1.408(5)	C9	C8	1.379(5)
C12	C7	1.355(8)	C9	C10	1.359(9)
F5	C10	1.359(4)	C7	C8	1.433(7)
N1	N2	1.265(3)	C2	C3	1.380(5)
N1	C7	1.411(5)			

Table S3. Bond Angles for APFA.

Atom	Atom	Atom	Angle/°	Atom	Atom	Atom	Angle/°
N2	C1	C2	127.5(4)	F3	C6	C5	116.4(5)
C6	C1	N2	116.8(5)	C5	C6	C1	126.6(5)
C6	C1	C2	115.7(3)	C12	C7	N1	131.0(4)
N3	C12	C11	115.9(5)	C12	C7	C8	116.3(4)
C7	C12	N3	121.9(4)	N1	C7	C8	112.6(5)
C7	C12	C11	122.2(5)	F4	C8	C9	119.2(4)
N2	N1	C7	114.5(3)	F4	C8	C7	118.4(4)
C10	C11	C12	118.1(5)	C9	C8	C7	122.4(5)
N1	N2	C1	116.8(4)	F1	C2	C1	119.6(3)
C6	C5	C4	114.6(5)	F1	C2	C3	120.9(5)
F2	C4	C5	117.4(4)	C3	C2	C1	119.5(4)
F2	C4	C3	117.8(5)	C4	C3	C2	118.8(5)
C3	C4	C5	124.7(4)	F5	C10	C9	117.9(5)
C10	C9	C8	117.3(5)	C11	C10	F5	118.4(5)
F3	C6	C1	117.0(4)	C11	C10	C9	123.6(4)

Table S4. Hydrogen-bond geometry (Å, °) for APFA.

D–H···A	D–H / Å	H···A / Å	D···A / Å	D–H–A / °
N3–H3A···N2	0.86	2.14	2.696(6)	121.8